Loughborough University

This item was submitted to Loughborough's Research Repository by the author.
Items in Figshare are protected by copyright, with all rights reserved, unless otherwise indicated.

Physical structuring of injectable polymeric systems to controllably deliver nanosized extracellular vesicles

PLEASE CITE THE PUBLISHED VERSION

https://doi.org/10.1002/adhm.201801604

PUBLISHER

© Wiley

VERSION

AM (Accepted Manuscript)

PUBLISHER STATEMENT

This is the peer reviewed version of the following article: NIKRAVESH, N. ... et al, 2019. Physical structuring of injectable polymeric systems to controllably deliver nanosized extracellular vesicles. Advanced Healthcare Materials, 8 (9), 1801604, which has been published in final form at https://doi.org/10.1002/adhm.201801604. This article may be used for non-commercial purposes in accordance with Wiley Terms and Conditions for Use of Self-Archived Versions.

LICENCE

CC BY-NC-ND 4.0

REPOSITORY RECORD

Nikravesh, Niusha, Owen Davies, Ioannis Azoidis, Richard J. Moakes, Lucia Marani, Mark Turner, Cathal J. Kearney, Neil M. Eisenstein, L.M. Grover, and Sophie C. Cox. 2019. “Physical Structuring of Injectable Polymeric Systems to Controllably Deliver Nanosized Extracellular Vesicles”. Loughborough University. https://hdl.handle.net/2134/37413.

Physical Structuring of Injectable Polymeric Systems to Controllably Deliver Nanosized Extracellular Vesicles

Niusha Nikravesh, Owen G. Davies, Ioannis Azoidis, Richard J. A. Moakes, Lucia Marani, Mark Turner, Cathal J. Kearney, Neil M. Eisenstein, Liam M. Grover and Sophie C. Cox*

N. Nikravesh: Laboratory for Particles-Biology interactions, Swiss Federal Laboratories for Materials Science and Technology (Empa), St. Gallen, 9014, Switzerland.

R. J. A. Moakes, I. Azoidis, N. M. Eisenstein, L. M. Grover and S. C. Cox: School of Chemical Engineering, University of Birmingham, Edgbaston, Birmingham, B15 2TT, UK

O. G. Davies and L. Marani: School of Sport, Exercise and Health Sciences, Loughborough University, Epinal way, LE11 3TU, UK

M. Turner: School of Sport, Exercise and Health Sciences, Loughborough University, Epinal way, LE11 3TU, UK; University Hospitals of Leicester NHS Trust, Infirmary Square, Leicester, LE1 5WW, UK

C. J. Kearney: Dept. of Anatomy, Kearney Lab & Tissue Engineering Research Group (TERG), Royal College of Surgeons in Ireland (RCSI), Dublin, Ireland; Trinity Centre for BioEngineering (TCBE), Trinity College Dublin (TCD), Dublin, Ireland; Advanced Materials and BioEngineering Research (AMBER), RCSI & TCD, Dublin, Ireland

* Corresponding author, Email: s.c.cox@bham.ac.uk

Abstract

Extracellular vesicles (EVs) are emerging as a promising alternative approach to cell-therapies. However, to realise the potential of these nanoparticles as new regenerative tools, healthcare materials that address the current limitations of systemic administration need to be developed. Here, two technologies for controlling the structure of alginate based microgel suspensions were used to develop sustained local release of EVs, *in vitro*. Microparticles formed using a shearing technique were compared to those manufactured using vibrational technology, resulting in either anisotropic sheet-like or spheroid particles, respectively. EVs harvested from pre-osteoblasts were isolated using differential ultracentrifugation and successfully loaded into the two systems, whilst maintaining their structures. Promisingly, in addition to exhibiting even EV distribution and high stability, controlled release of vesicles from both structures was exhibited, *in vitro*, over the 12 days studied. Interestingly, a significantly greater number of EVs were released from the suspensions formed by shearing (69.9±10.5%), compared to the spheroids (35.1±7.6%). Ultimately, alterations to the hydrogel physical structures have shown to tailor nanoparticle release whilst simultaneously providing ideal material characteristics for clinical injection. Thus, the sustained release mechanisms achieved through manipulating the formation of such biomaterials, provide a key to unlocking the therapeutic potential held within EVs.

1 Introduction

Extracellular vesicles (EVs) are biological nanoparticles with lipid bilayers comprising of cytoplasmic and membrane proteins as well as nucleic acids, including mRNA and miRNA.[1] EVs are released from most cell types under physiological as well as pathological conditions and can be categorised into three subtypes: exosomes, microvesicles (or shedding vesicles), and apoptotic bodies.[2, 3] These subgroups are distinguished by size, biogenesis, and to some extent by their protein markers. The release of exosomes (30 - 150 nm) into the extracellular environment occurs through the endocytic pathway, while microvesicles (100 - 1000 nm) are generated by outward budding or blebbing from the cell's plasma membrane. Finally, apoptotic bodies with broad size range (100 - 5000 nm) are released from dying cells and contain multiple, densely packed, organelles.[1, 2, 4]

EVs have been shown to have roles in cell-cell interactions and important biological processes such as immunomodulation, cancer progression, angiogenesis, and tissue regeneration.[5, 6] More specifically, the effective role of vesicles derived from mineralising osteoblasts and mesenchymal stem cells has been demonstrated for bone regeneration and regulation of osteogenesis.[7, 8] The repair of bone defects remains a huge demand within modern medicine. The possibility of stimulating osteoblasts *in vitro* to produce vesicles programmed to promote osteogenesis, or other regenerative processes, when delivered locally to the site of a defect presents an exciting new approach to solving this growing challenge. One of the great potential advantages of the therapeutic application of cell-derived vesicles is that this technology may overcome some of the complications associated with cell-based therapies, including malignant stem cell transformation, and nutrient as well as oxygen deprivation at the recipient site, which can significantly affect cell survival rates.[9-11] Another strength of the therapeutic application of EVs is their potential to be generated *in vitro* under defined conditions. If this could be achieved at scale, then this may present significant economic and regulatory advantages compared with the use of stem cells.

There are, however, currently two major obstacles for the therapeutic application of vesicles. Firstly, scaling at a reproducible and cost-effective level is still unfounded, restricted by large-scale isolation in sufficient quantities of '*active*' vesicles.[5, 12] The second obstacle is targeting EVs to a specific therapeutic location and maintaining an efficacious dose at that site so that localised pathologies, such as bone diseases or tumours, may be treated. Previous studies have demonstrated rapid uptake of vesicles by organs, such as the lungs and liver due to aggregation and recognition by the reticuloendothelial system. *In vivo* studies for monitoring the distribution of systematically administered cell-derived vesicles based on the application of fluorescent imaging techniques, fails to prove targeted delivery of these effective nanoparticles to specific tissues.[9, 12-15] As such, the incorporation of vesicles into delivery devices for the treatment of localised pathologies presents the opportunity for controlled release thus overcoming the issues with systemic administration. Additionally, the development of such systems may prove advantageous on multiple fronts including, delivery of nano-therapies within the field of cancer treatment [16], reduction in dosages through enhanced bioavailability and unlocking the potential of EVs for the tissue engineering and biomaterials communities.

The use of injectable synthetic or natural polymeric biomaterials present opportunities to tailor release by altering physicochemical properties.[17] Specifically, alginate, a polysaccharide with the ability to undergo gelation *in situ*, has gained much interest in recent years within drug delivery and regenerative medicine.[18-21] Alginate's ability to undergo gelation *in situ* arises through its chemical structure, with repeating blocks of mannuronic and guluronic acid residues resulting in an "egg-box" gelation mechanism; divalent crosslinking of homopolymeric regions of guluronic acid residues, using Ca^{2+} ions.[22] Recently, much attention has been given to restructuring hydrogel matrices, with a view to manipulating the microstructure and subsequent bulk properties, including release of various biomolecules.[23] As such, processing technologies such as applying shear have been employed to ultimately confine the gelation process, restricting gel formation to result in suspensions of microparticles. Bulk properties

(viscosity, moduli, etc.) have been shown to be a function of the gelation kinetics; whereby an equilibrium between polymerisation and shear breakdown results in weak inter-particle interactions, forming weak gel-like networks at rest that flow under applied deformation.[24] In these cases, entrapment is achieved via several mechanisms: firstly, becoming trapped within the gelled phases and/or, secondly, becoming trapped within the interstitial regions between particles. In comparison, encapsulation technologies, such as vibrational nozzle, form droplets by forcing an alginate sol through an orifice, leading to entrapment of moieties solely within the gel due to rapid curing. Release of these trapped molecules is governed by factors such as polymer concentration and crosslink density.[25]

This research seeks to control EV release kinetics in a sustained manner with the potential to facilitate local delivery for the treatment of contained pathologies. In this paper we compare two processing methods that result in different degrees of EV confinement by employing either shear or vibration to form micro-particulate suspensions with varying intrinsic properties. To assess the suitability of these different systems for localised EV release this paper covers: (1) manufacture and characterisation of the microgel suspensions as a minimally invasive delivery system; (2) evaluation of vesicle stability through processing and cytotoxicity; and (3) a comparison of the *in vitro* release of vesicles from the two structured systems. Notably, the EV population used in this study was isolated from osteoblasts grown under osteogenic conditions, which have been previously demonstrated to exhibit the capacity to induce stem cell mineralisation beyond that of the current gold standard treatment (bone morphogenetic protein-2 (BMP-2)).[7] Therefore, to the best of our knowledge, this is the first attempt to use biomaterials to control the local release of regenerative cell-derived vesicles. Overall, this paper highlights the promise for cell-derived vesicles to be utilised as biological, but acellular, regenerative tools that could be employed to treat a range of local pathologies, including cancer and musculoskeletal defects.

2 Materials and methods

2.1 Cell culture

MC3T3 pre-osteoblasts (ATCC CRL-2593, UK; passage number < 10) were cultured in Minimum Essential Medium (alpha-MEM; Sigma, UK) supplemented with 10% fetal bovine serum (FBS; Sigma, UK), 2 mM L-glutamine (Sigma, UK), and 1% penicillin/streptomycin (Sigma, UK). All cultures were incubated at 37°C with 5% CO_2 until they reached 70-80% confluence. Culture medium was changed every other day to enhance cell growth and viability.

2.2 EV isolation

MC3T3s were expanded in T-175 cm^2 flasks in osteogenic medium, which was prepared by the addition of 50 µg/mL L-ascorbic acid (Sigma, UK) and 10 mM ß-glycerophosphate (Sigma, UK) to exosome-depleted growth medium. For the preparation of osteogenic medium, exosome-depleted FBS was prepared by ultra-centrifuging the serum for 16h at 120,000 g.[7] Cells were grown for two weeks, and osteoblast-derived EVs isolated from the conditioned culture medium using a differential ultracentrifugation method. Briefly, the conditioned media was centrifuged at 2,000 g for 20 min to remove cell debris. The supernatant was then centrifuged at 10,000 g for 30 min, followed by ultra-centrifugation (Sorvall WX Ultra Series; Thermo Fisher, UK) (Rotor: Fiberlite, F50L-8 × 39 fixed-angle rotor; Piramoon Technologies Inc., USA) at 120,000 g for 70 min. For further purification, the pellet was washed in sterile filtered phosphate buffer saline (PBS; Sigma, UK) at 120,000 g for 70 min.[7, 26] All centrifugation steps were performed at 4°C. The pellet was then re-suspended in 200 µL of PBS and stored at -20°C.

2.3 EV characterisation

Since the focus of this work is the polymeric systems, readers are directed to previous work that provides a full characterisation of the EVs used in this study, including proteomics. [10] However, since the purity of EVs is important within the field and to adhere with the minimal experimental requirements recommended by Lotvall *et al.* 2014, Western blots have been performed along with two techniques to characterise single vesicles; transmission electron microscopy (TEM) and nanoparticle tracking analysis (NTA).[27]

Western blotting analysis was used to confirm the presence of EV proteins. Following electrophoretic separation using precast 4-15% Mini-PROTEAN® TGX™ gels (Biorad), the gels were blotted onto PVDF membranes (Invitrogen) and blocked with 5% non-fat milk powder (Alix, Annexin A2 and TSG1010) or 2% non-fat milk powder (CD63) in Tris-buffered saline. After 1 hour blocking at room temperature, the membranes were incubated with primary antibodies in their respective blocking buffers overnight at 4°C at a dilution of 1:1000 (Alix, Annexin A2 and TSG1010) and 1:500 (CD63) in Tris-buffered saline containing 0.5% Triton X 100. After three washes, the blots were incubated with 1:2000 horseradish peroxidase-conjugated secondary antibodies for 1 hour at room temperature. Chemiluminescence detection of bands was performed with ECL Plus reagent (Biorad).

TEM was performed using negative staining for which 5 µl of EV sample was absorbed on a continuous carbon-coated copper grid (Agar Scientific). Then the sample was stained with UranyLess EM (CN Technical Services, Ltd.) followed by lead citrate (CN Technical Services, Ltd.). All the steps were performed on drops of a parafilm. The grids were left to dry before being visualised on a JEOL 2100, 200 kV LaB6 TEM. Micrographs were acquired in RADIUS 2.0 (Build 14402) software using a MegaView G3 (Olympus Soft Imaging Solutions) camera at a resolution of 1776 x 1456.

Vesicles suspended in PBS were analysed by NTA using the Nanosight LM10 (Malvern Instruments Ltd, UK) utilising a 455 nm laser. Based on Brownian motion, EV size and concentration was calculated using accompanying software (version 3.2). For all samples, ambient temperature was set to 22°C and camera level and detection threshold were adjusted

between 12-15 and 3-7, respectively. For each sample, five videos of 30 second duration were recorded. The number of completed tracks per sample was > 500.

2.4 Preparation of encapsulation solutions

Medium viscosity alginate (ALG; ≥20,000 cP, M/G ratio=1.56) from brown algae (Sigma, UK) was used to manufacture microgel suspensions. 1% and 2% w/v alginate solutions were prepared in sterile deionised water while the solution was heated to 90°C under stirred conditions for two hours. Cross-linking solutions (0.1 and 0.2 M) were prepared by dissolving granular calcium chloride (Sigma, UK) in deionised water. All solutions were sterile filtered using 0.22 μm syringe filter (Millipore, USA) and left under a UV light overnight.

2.5 Preparation of alginate microgel suspension

A range of sheared microgel suspensions with formulations obtained through design of experiments were produced as detailed in Table 1. An overhead stirrer equipped with pitch blade impeller was used to provide the shear field required for the formation of the sheared microgel suspensions (fig. 2b). The cross-linker ($CaCl_2$) was slowly added to the alginate sol at the impeller tip, in order to form the hydrogel particles within the turbulent regime. After the addition of the cross-linker, systems were further mixed for 10 min, and then degassed using a sonicator for 15 min to remove any trapped air. The entire gelation process was performed at room temperature, and each formulation was made in duplicate to assess reproducibility. All fluid gels were stored at 4°C for 24h before being used for rheological studies. Encapsulation of EVs was undertaken at room temperature by suspending EVs (5.6×10^9 particles/ml) in the alginate solution prior to crosslinking.

Table 1: Design of experiments to assess the effect of alginate concentration, cross-linker concentration, the volumetric ratio between the polymer and the cross-linker, and the magnitude of shear field on microgel suspension rheology

Alginate Concentration (%w/v)	$CaCl_2$ Concentration (M)	$CaCl_2$ / Alginate (%v/v)	Agitator Speed (RPM)
1	0.1	7.5	300
1	0.1	15	300
2	0.1	6	300
2	0.1	9	300
2	0.1	12	300
1	0.2	6	300
2	0.2	4	300
2	0.2	6	300
2	0.2	9	1200
2	0.2	8	1200
2	0.2	6	1200

2.6 Preparation of alginate spheroidal microparticles

EVs at a concentration of 5.6 $x10^9$ particles/mL were suspended in sterile 1%w/v alginate solution. The microparticles were generated using a vibrational nozzle encapsulator (A B-395 pro, Buchi, UK) under sterile conditions.[25] The generated droplets were incubated in a crosslinking solution (0.1 M $CaCl_2$) located at 20 cm from the nozzle head for 10 min (fig. 2c). The encapsulator parameters were: nozzle inner diameter = 200 µm, frequency = 6000 Hz, electrode = 1200 V, and pump flow rate = 40 mL/min. The generated spheroidal microparticles were then filtered and subjected to several washes with PBS to remove any remaining unbound calcium ions. The size distribution of 20 randomly selected alginate microparticles were then determined using a light microscope (Olympus Co., Germany) and Image J software (NIH, Bethesda, MD, USA).

2.7 Rheological characterisation

Manufactured alginate sheared microgel suspensions were evaluated using an AR-1000 rheometer (TA Instruments, UK) fitted with a stainless-steel cone and plate geometry (cone angle of 2 ° and diameter of 40 mm). An oscillatory sweep (frequency sweep), and flow curve (viscosity versus shear rate) at a constant temperature of 37 °C were performed. Small

deformation rheology was undertaken by varying the frequency applied to the gel (0.01 to 10 Hz) at a constant strain determined to be within the linear viscoelastic region (0.5%). Dynamic viscosity measurements were conducted between 0.1 to 1000 s^{-1} in rate controlled mode. A toothpaste sample was used as a positive control for this study since this product exhibits controllable flow behaviour and desirable recovery characteristics following application of shear stress. Furthermore, the use of a readily available product presents the opportunity for others in the field to easily conduct comparative studies.

2.8 Live/dead assay

The cytocompatibility of the optimised sheared microgel suspension composition was examined using a live/dead cytotoxicity assay (Invitrogen, UK). Briefly, MC3T3s ($2x10^5$ cells/mL) were seeded on the top of transwell plate (fig. 4). After 4h of incubation, the sheared microgel suspension was placed on the top of the transwell insert (pore size: 0.4 µm) and cells were incubated at 37 °C for 48 h. On the day of the experiment 5 µL of calcein AM (live cell marker; Ex: 495 nm; Em: 515 nm) and 25 µL of propidium iodide (PI; dead cell marker; Ex: 488 nm; Em: 617 nm) were added to 2 mL of growth medium (alpha-MEM supplemented with 10% v/v foetal bovine serum).[28] Cells were then incubated in the dark at 37 °C for 15 min. Stained cells were visualised using confocal laser scanning microscopy (Olympus FV1000, Multiple Ar laser, Germany). For the control, the viability of cells without gel was examined.

2.9 Labelling of EVs with fluorescent dyes

To investigate the integrity of vesicles during sheared microgel suspension formation, isolated EVs were stained with two fluorescent dyes. The lipid membrane and RNA cargo of EVs were stained using FM1-43FX [29, 30] (Ex: 479 nm; Em: 598 nm), and SYTO RNA Select (Ex: 488 nm; Em: 530 nm), respectively according to the manufacturer's instructions (Life technology, UK). Briefly, prior to encapsulation, EVs were stained with the RNA dye at a final concentration of 10 µM and incubated at 37 °C for 20 min. Labelled EVs were then washed twice in PBS

using ultracentrifugation at 120,000 g for 70 min. For the lipid dye, the EVs were stained with a final dye concentration of 5 μg/mL. The stained EVs were incubated at room temperature for 10 min and were then washed in PBS. A confocal microscope was used to visualise fluorescently-labelled samples at 10x magnification. Reconstruction of raw z-stack images of 3D gels were achieved using Imaris software (Bitmap, UK). Further studies were performed by measuring the amount of co-localisation between the two dyes using Image J (coloc.2 plugin). Numerical data were evaluated by Pearson's correlation coefficient (R-value) for which a value of 1 represents a perfect linear correlation and values above 0.7 indicate a strong correlation.[31, 32] To obtain accurate co-localisation results, acquired micrographs had low noise level, and the same point spread function was applied for both green and red channels. Additionally, for evaluating the number of encapsulated EVs within focal planes of the alginate sheared microgel suspension and microparticles a spot-detector plugin from Imaris software was employed.

2.10 Release studies from alginate systems

In vitro release profiles of EVs from both alginate structures were carried out by direct dispersion method.[33, 34] Loaded alginate sheared microgel suspensions and microparticles were each suspended in 2 mL of sterile filtered PBS and incubated at 37 °C. The receiving medium was sampled (300 μL) from each system at regular time intervals and was immediately replaced by an equal amount of fresh PBS. The collected samples were then assayed to quantify EV release.

For the short-term release studies (1, 3, and 5 h), the concentration of released particles in the receiving medium was measured using NTA. This analysis was used as an initial indication of any release and to compare size profiles with those of EVs before incorporation into the alginate systems. To ascertain whether particles detected by NTA were in fact EVs, an ExoELISA-ULTRA complete kit was used to assay the media from long-term release studies (1, 3, 6, and 12 days). This further analysis indicated the concentration of CD63 positive

particles, a known EV surface marker, that were released from the systems which were compared with NTA results. The cumulative percentage released from hydrogels at each time point was determined by considering the dilution effect, and all experiments were performed in duplicate. Further, for both assays control samples of void spheroid microparticles and microgel suspension were also evaluated and no release was detected by via NTA or ExoELISA.

2.11 Statistical analysis

Graphs and statistical analyses were performed using Prism-7 software (Graph Pad, San Diego, CA). Results are presented as the mean ± standard error of the mean (SEM). One-way analysis of variance (ANOVA) was used to identify any significant difference between the means of independent groups. Furthermore, a Bonferroni post-hoc test was performed with ANOVA to find means that were significantly different between groups. A p-value < 0.05 was considered as significant.

3 Results

3.1 Characterisation of osteoblast derived EVs

Despite the focus on this manuscript being the release of EVs from injectable biomaterials, it was important to first demonstrate purity. Characterisation was conducted following guidelines published by the International Society for Extracellular Vesicles.[27] Western blots confirmed the presence of ISEV designated markers, Alix (97 KDa), CD63 (50-60 KDa), TSG101 (45-50 KDa) and Annexin A2 (37 KDa) (fig 1a). A typical spheroid morphology was demonstrated using TEM (fig 1b) with an average size of 186±4 nm confirmed by NTA (fig 1 c). Based on the size of isolated vesicles they are non-specifically referred to as extracellular vesicles, which demonstrates a mixed population, likely consisting of exosomes and micro vesicles. It

is also notable that micrographs of these osteoblast derived EVs revealed a relatively high electron density, as was confirmed previously by our team.[7]

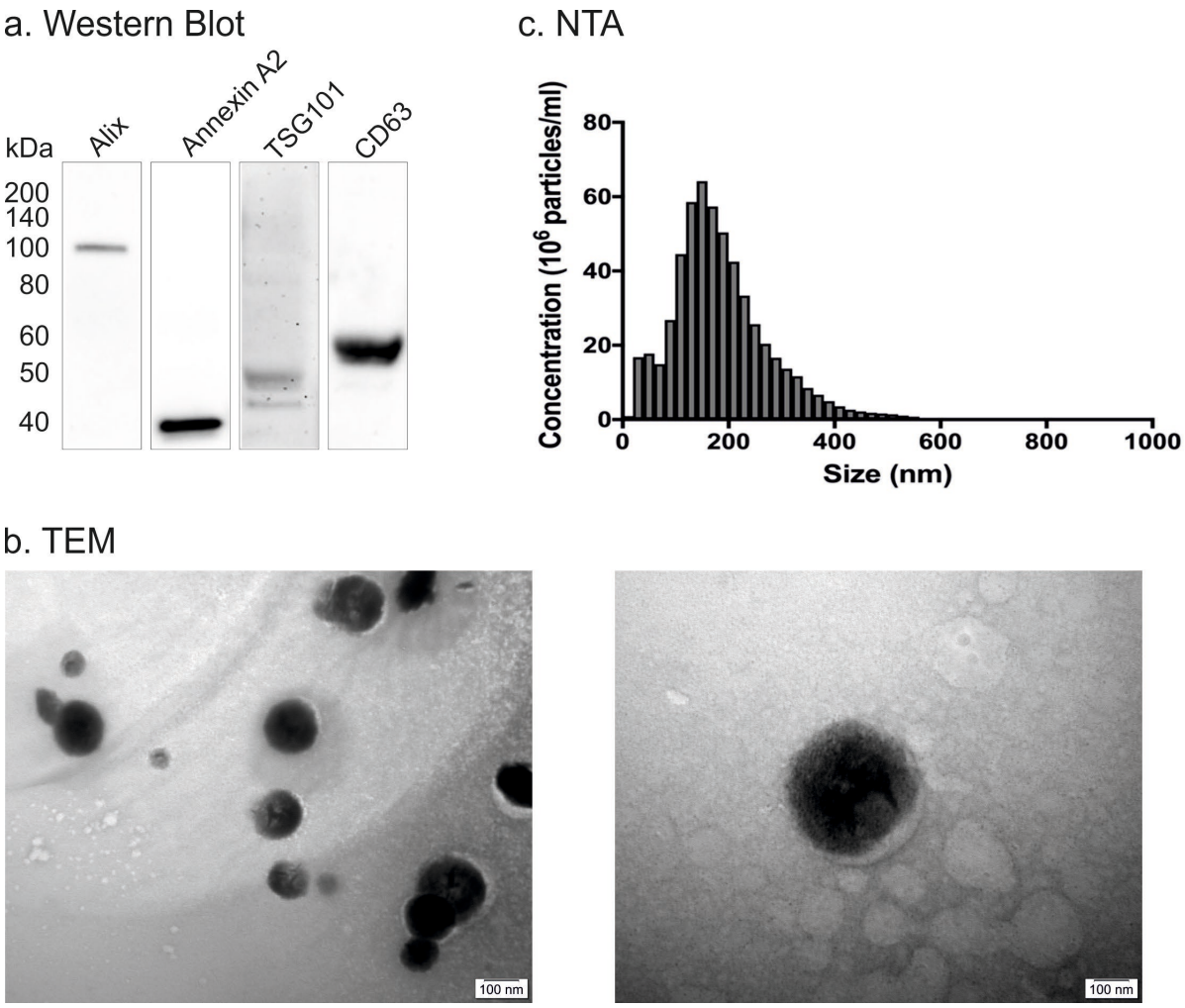


Fig 1. Characterisation of EVs. (a) Western blot analysis of common EV markers (Alix, Annexin A2, TSG101 and CD63). A total of 5 μg of protein was loaded for Alix, Annexin A2 and TSG101. 20 μg of protein was loaded for CD63. (b) Micrographs demonstrating typical spheroidal morphology of EV population (left) and electron density of single vesicle (right). (c) Particle size distribution of EV sample extracted from nanoparticle tracking analysis (NTA) indicating an average size of 186±4 nm.

3.2 Formulation and characterisation of EV loaded microgel suspensions

3.2.1 Microparticle size, shape and EV distribution

Light microscopy was used to evaluate both particle size and shape following either shear or vibration processing. Figure 2 shows the change in particle morphologies as a function of the

confinement technique used during the sol-gel transition, with sheared systems forming large anisotropic particles (fig. 2a) and vibrational systems exhibiting spheroidal shape (fig. 2b). The alginate micro-particles generated using vibrational technology exhibited a high degree of homogeneity, with an average diameter of 364 ± 6 μm. However, irregular shape and distribution of particles made it difficult to size the sheared systems in this way.

In order to investigate the distribution of the encapsulated EVs within the two microgel suspensions, the lipid membrane of EVs were stained with a fluorescent dye (FM1-43FX) before encapsulating. Confocal microscopy demonstrated an even distribution of EVs within both alginate systems (fig. 2c). In the case of the spheroids, EVs were distributed throughout the particles only. In contrast, for the sheared systems, EVs were evenly observed across the whole volume studied, irrespective of particle shape and distribution. Quantitative evaluation of 3D reconstructed micrographs revealed an average of 1226 ± 21 and 1114 ± 53 EVs per 1000 μm for the sheared and spheroidal micro-particles, respectively. Thus, confirming that the number of EVs incorporated in both physically structured systems were similar. Some aggregation of EVs was found to occur in both sheared and spheroids, which is not remarkable given their size. Notably, no fluorescent signal was detected in control samples without EVs (this image is not shown since it was entirely black).

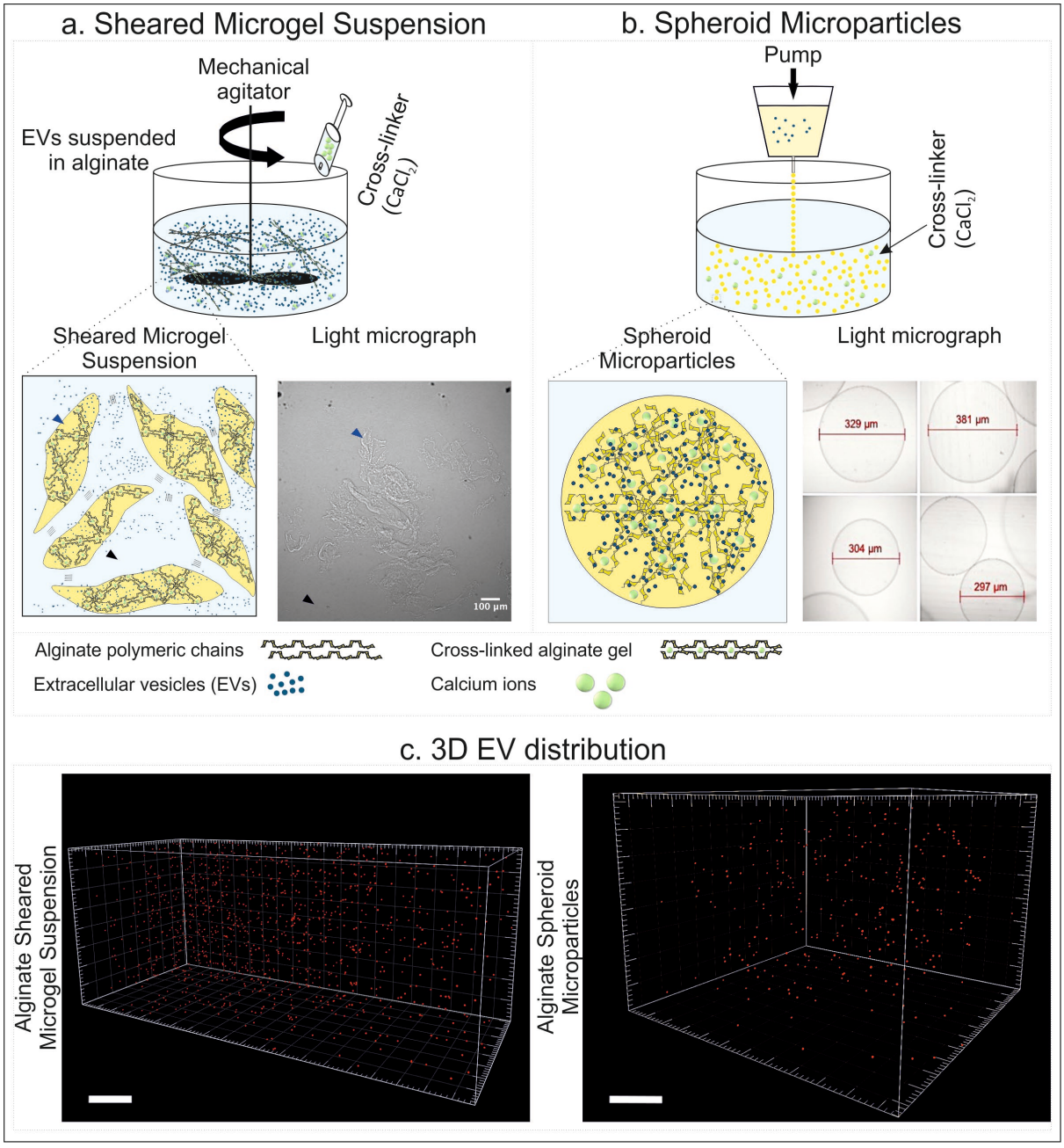


Fig 2. Schematic representation the manufacturing process for both EV loaded systems, highlighting the resultant structures. (a) Manufacturing set-up for an alginate microgel suspension (2%w/v alginate, 0.2 M $CaCl_2$, and 6% v/v) and resulting physical structure. (b) Production of spheroid alginate microparticles using vibrational technology (nozzle inner diameter: 200 µm, frequency: 6000 Hz, electrode: 1200 v, pump flow rate: 40 mL/min) and images highlighting final homogeneous gel structure. (c) 3D visualisation of encapsulated vesicles within the sheared microgel suspension and spheroid microparticles; vesicles were labelled with FM1-43FX before encapsulation; scale bars show 100 µm (particles radius scale: 2)

3.2.2 Rheological characterisation and injectability

It is important to recognise that processing parameters play an important role in resultant particle diameters, distribution and shape,[35] factors which all ultimately influence the clinical applicability and release kinetics of loaded actives. For spheroid microparticles formed via the vibration method the alginate concentration, flow rate and vibrational frequency were optimised such that the solution jet broke up into uniform droplets (364 ± 6 μm).

In the case of the sheared systems, multiple formulations and process parameters were investigated in order to assess any influence on key rheological properties (fig. 3). All of the manufactured samples were found to exhibit shear-thinning behaviour (fig. 3a). Application of a higher agitator speed (1200 rpm) during processing, as well as increased polymer (2% w/v) and cross-linker (0.2 M) concentrations, resulted in a shift in flow profiles towards that of the positive control, toothpaste.

Following these initial findings, the viscoelasticity of two compositions, containing different ratios of polymer to crosslinker (8% v_{CaCl2}/v_{ALG} and 6% v_{CaCl2}/v_{ALG}), was assessed. Small deformation rheology was conducted over a range of frequencies (from 0.1 to 10 Hz), at a constant physiological temperature, in order to probe gel-like behaviours at rest - post-injection. Figure 3b shows the mechanical data obtained for both storage modulus (G') and loss modulus (G") as a function of frequency, for both sheared systems in comparison to the control. Sheared systems displayed a small degree of frequency dependency, typically lying between a strong and weak gel. Such observations are commonly noted for such systems as interactions between the particles give rise to a weak elastic network.[36] Suspensions formulated with a lower salt to polymer ratio, 6% $v_{CaCl2}/v_{ALG,}$ exhibited lower G' and G'' values, more similar to the control. The injectability data also demonstrated that the sheared systems with 6% v_{CaCl2}/v_{ALG} were easier to inject, as indicated by an overall lower maximum force (3.8 N versus 4.3 N) experienced during extrusion (fig. 3c). Therefore, based on rheological

studies, the sheared microgel suspension with 2% w/v alginate, 0.2 M $CaCl_2$, and 6% v/v was further investigated for the encapsulation/release of osteoblast-derived vesicles.

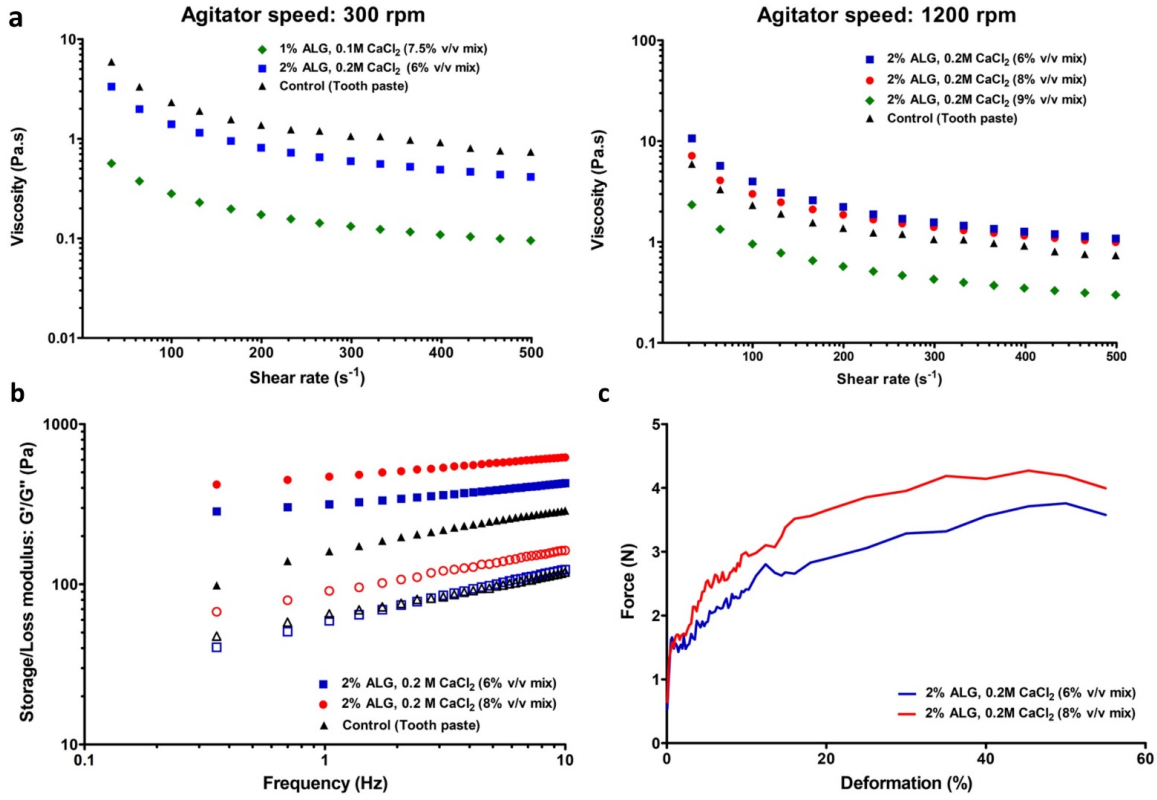


Fig 3. Rheological characterisation of alginate sheared microgel suspensions at 37 °C. (a) Viscosity profiles for the sheared microgel suspensions processed at both 300 rpm and 1200 rpm stirrer speeds. (b) Frequency sweeps obtained at 0.5% strain dependence, closed markers denote storage modulus (G') and open, loss modulus (G''). (c) Injectability data showing the force required to expel the formulations through a 21G needle

3.3 EV stability throughout processing and microgel cytotoxicity

3.3.1 Evaluation of lipid membrane and RNA co-localisation for encapsulated vesicles

The degree of co-localisation of fluorescently labelled membrane lipid and RNA cargo was investigated as a tool to assess if the EVs were intact post-encapsulation. Statistical analysis of confocal micrographs confirmed a high degree of co-localisation between the two dyes, as indicated by an R-value greater than 0.7 (R = 0.819 ± 0.06), suggesting the EV cargo and membrane were largely still associated following processing. Images in Figure 4 are from the

sheared microgel suspensions and similar trends were observed for the spheroidal microparticles (not shown). Again, some aggregation of EVs were witnessed.

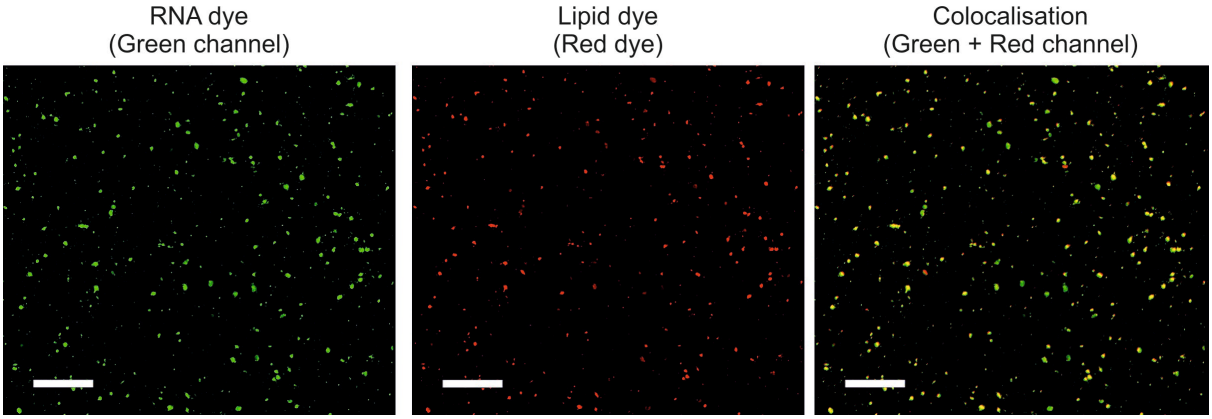


Fig 4. Visualisation of fluorescently stained vesicles utilising confocal scanning microscopy. Co-localisation analysis: encapsulated vesicles following incubation with RNA probe (SYTO RNA Select, green channel) and lipid dye (FM1-43FX, red channel); scale bars show 50 μm.

3.3.2 Microgel cytotoxicity

To determine whether the optimised sheared alginate microgel suspension had any adverse effect on cell viability, MC3T3 pre-osteoblasts were cultured in the presence and absence of the formulation. Confocal images acquired after 48h revealed a similar degree of cell viability between the control and those exposed to the sheared microgel suspension (fig. 5). The results suggest that cell viability remained close to 100% for both groups.

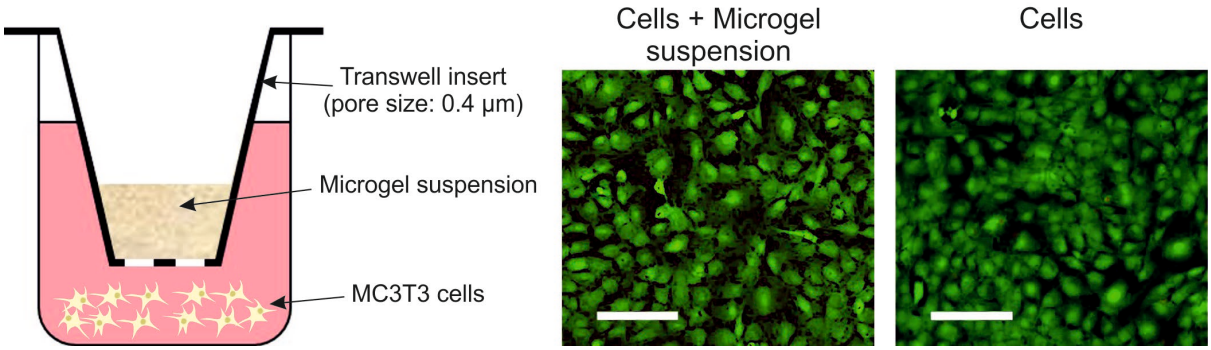
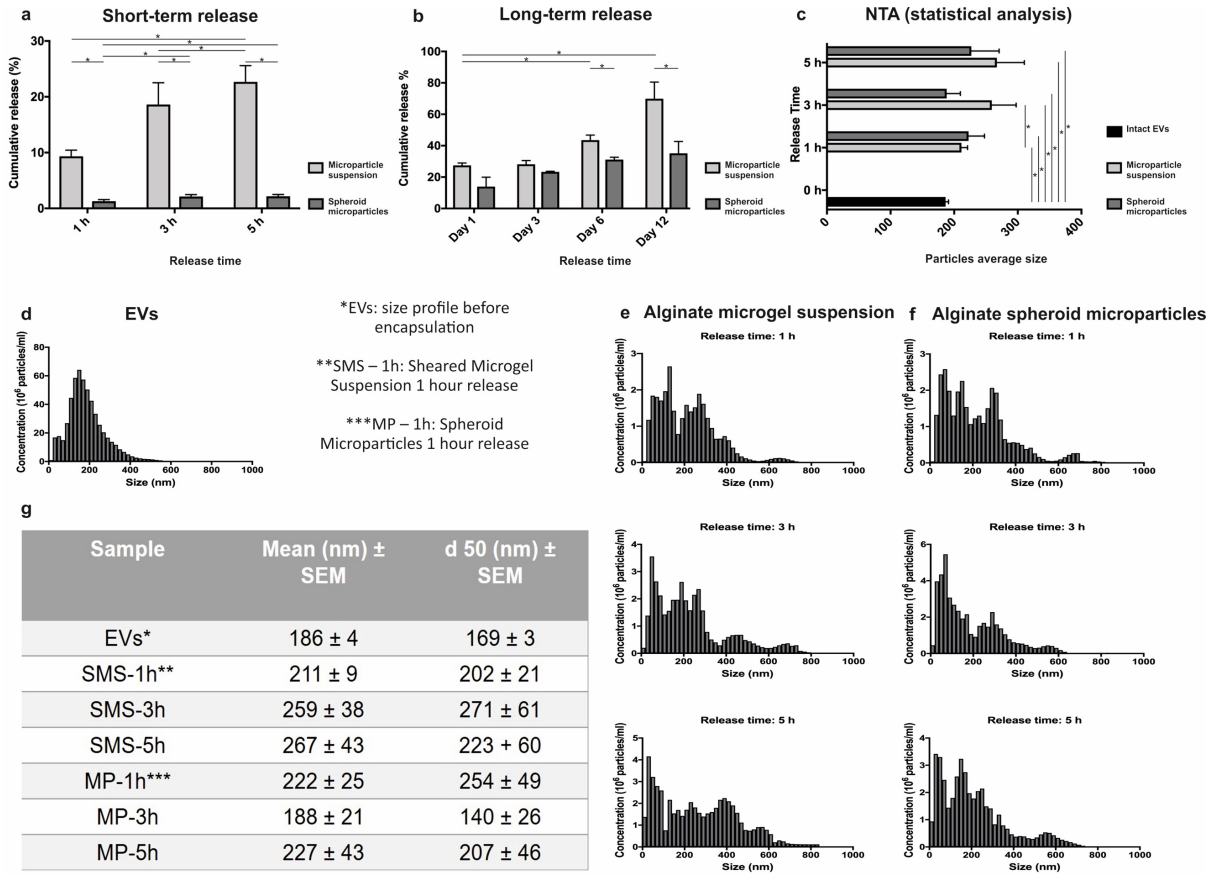


Fig 5. Visualisation of microgel cytocompatibility utilising fluorescence. Two-dimensional confocal micrograph of live pre-osteogenic cells (MC3T3s) in contact with optimised alginate sheared microgel suspension formulation (2% ALG, 0.2 $CaCl_2$, 6 %v/v) using transwell plate culturing method (calcein AM marker: green channel); scale bars show 100 μm.

3.4 EV release from microgel suspensions

All *in vitro* release studies were performed in PBS at pH=7.2. Short-term release studies, up to 5 hours (fig. 6a), were conducted using NTA to assay elution media for particles. After 1, 3, and 5h, cumulative releases of 9.3±1.1%, 18.62±3.8%, and 22.7±2.9% was measured, respectively, from the sheared system, demonstrating a gradual release during the first few hours (fig. 6a). For the alginate spheroids, after 5h the cumulative release was found to be only 2.2±0.3% (fig. 6a).



g

Sample	Mean (nm) ± SEM	d 50 (nm) ± SEM
EVs*	186 ± 4	169 ± 3
SMS-1h**	211 ± 9	202 ± 21
SMS-3h	259 ± 38	271 ± 61
SMS-5h	267 ± 43	223 + 60
MP-1h***	222 ± 25	254 ± 49
MP-3h	188 ± 21	140 ± 26
MP-5h	227 ± 43	207 ± 46

Fig 6. Evaluation of vesicles release from alginate sheared versus spheroidal microparticles. (a) Short and (b) long term cumulative release profiles for vesicles in PBS. (c) Statistical comparison between the average size (nm) of intact and vesicles released from both the sheared microgel systems. (d) Size distribution of intact (non-encapsulated) vesicles determined by nanoparticles tracking analysis (NTA) (Note, this data is also represented in fig 1c but repeated here to enable direct comparison). (e) and (f) Average histogram plotted with NTA reports representing size distribution of released vesicles from sheared and spheroidal microparticles over 1h, 3h, and 5h. Error bars show ± SEM. (g) Mean and median diameter (d_{50}) of both non-encapsulated and encapsulated vesicles obtained from NTA.

Longer-term release studies (up to 12 days) were determined based on CD63 antigens, a tetraspanin protein known to be associated with the membrane of cell-derived vesicles. Figure 6b shows that 27.42±1.6% of CD63 positive EVs were released from the sheared alginate system after 24h, increasing to 69.88±10.5% over the following 12 days. Notably, a lower cumulative release of 13.87±6% after 24h ($p= 0.081$) and 35.10±7.55% after 12 days ($p=0.015$) was observed from the alginate spheroids (fig. 6b). This trend was in agreement with results obtained from short-term release studies.

Interestingly, Figure 6c demonstrates statistically significant differences between the average size of freshly isolated EVs (fig. 1c/6d), and particles released from the developed systems at each time point. Despite the different hydrogel structures, no statistical difference ($p > 0.05$) between the average size of released EVs from sheared microgel suspensions and spheroidal particles were detectable (fig. 6c). Although, notably at 5 hrs there appeared to be a greater portion of EVs >300 nm eluted from the sheared microgels, suggesting that diffusion of larger aggregates was hindered in the spheroid networks (fig. 6e and f).

4 Discussion

Over the last decade, cell-derived EVs have been shown to play a critical role in cellular communication and tissue regeneration. To date, systemic delivery of EVs has been the only method studied for the administration of isolated vesicles within biological systems.[37, 38] However, *in vivo* studies have demonstrated that upon systemic delivery, EVs are sequestered within the first 30 min after injection by circulating macrophages mainly in the liver, spleen, kidneys, and lungs. Hence, strategies to achieve localised release of EVs may enable their promising therapeutic potential to be realised. Notably, there is significant literature that highlights local administration of nanoparticles at the therapeutic site may improve efficacy,[9, 38, 39] which presumably is extendable to EVs. The present study demonstrates for the first time the possibility to manipulate the physical structure of a popular biocompatible hydrogel, alginate, to produce injectable systems capable of releasing cell-

derived vesicles. We show that by altering the physical structure of the polymer, by applying two different processing techniques, it is possible to tailor the release of EVs in an *in vitro* model. While in this paper we have loaded these systems with EVs isolated from pre-osteoblast cells there would certainly be opportunities to incorporate vesicles derived from other cell types or even synthetic nanoparticles for the treatment of different pathologies, such as cancer.

Shearing during the sol-gel transition as a means to confine gelation into microparticles was compared to those formed using vibrational nozzle technology, an approach more commonly adopted in the literature. This resulted in very different suspension microstructures, with anisotropic and spheroidal homogeneous microparticles formed on shear and vibration, respectively. Particles in both cases were observed to be less than 700 μm (364 ± 6 μm in the case of spheroids), complying with injectable systems previously described for pharmaceutical reagents or cells.[41] Notably, particles produced using the vibrational nozzle technique resulted in narrow size distributions, compared with other microencapsulation techniques.[26, 42, 43] In our previous study, it was verified that a combination of experimental parameters, such as polymer flow rate, frequency, and polymer concentration can influence the average diameter, size distribution and shape of the produced microparticles, which can be manipulated to achieve a desired profile.[25] Here, we aimed for small particles to facilitate injection through smaller syringe needles, and provide a greater surface area to volume ratio for the diffusion of encapsulated vesicles into the surrounding environment.

Following manufacture of both alginate systems, it was important to determine the distribution of the EVs within the hydrogel matrices. Due to the small size of EVs imaging is reportedly difficult, as the nano-sized particles constantly moving under Brownian motion. However, in this study, the gelled structures provided a matrix which suppressed EV motion. As such, images were able to be taken over extended period, allowing 3D z-stacks to be obtained. 3D reconstructions (fig. 2c) highlighted homogenous distributions of the EVs across both microgel

systems, where, in the case of the spheroids restriction to the gelled phase can clearly be seen. In contrast, sheared systems exhibited uniform distributions indiscriminate of the gelled or surrounding aqueous phase. Such changes arise from the processing; where using vibration technology, rapid gelation as the drops enter the curing vat prevents diffusion of EVs into the aqueous phase at this time. However, imparting shear during the sol-gel transition inevitably causes some of the EVs to remain outside the gelled phase, becoming subsequently trapped between particles. In addition to using these hydrogels as a means to control EV release, immobilisation of nanoparticles within these systems may also facilitate imaging approaches.[40]

Taking the clinical application into consideration, minimally invasive techniques are advantageous due to their patient compliance. Release of EVs from a locally injected gel would be more acceptable to potential patients compared with more invasive open procedures. Injections, present a good way of locally delivering biomaterials that may release therapeutics. In order to guide what rheological behaviour would be desirable for an injectable therapeutic agent, we chose to use toothpaste as a positive control. This is because it is readily available, and exhibits shear thinning behaviour that enables easy injection (fig. 3). As such, a commercially available injectable product, toothpaste, was selected for baseline in which to compare material behaviours. Rheological characterisation under physiological conditions (pH = 7.2 and temperature 37°C) revealed that all formulations exhibited shear-thinning behaviour (fig. 3a). Such behaviour is desirable within injectable systems, lowering the magnitude of force required to administer the therapy. Furthermore, sheared systems showed weak solid-like viscoelastic characteristics at rest (fig. 3b). Again, such properties make it ideal for sustained release, providing a structure that remains stable post-injection without falling apart. Together the material behaviour allows the system to act like a liquid through the needle and then self-structuring *in situ* to provide a gel for controlled localised delivery. The 2%w/v alginate, 0.2 M $CaCl_2$ (6% v/v mixture) was found to give mechanical data closest to the ideal control, on this basis it was selected for further studies.

Processing conditions are key when designing delivery devices for sensitive therapeutics. During the manufacture and encapsulation processes, EVs are exposed to a high degree of mixing, and resultant shear forces. Thus, it is critical to evaluate the stability of EVs in the form of retained biological structure post-process. Promisingly, a high degree of co-localisation between the lipid membrane and internal RNA content (R-value: 0.819 ± 0.06) (fig. 4) was observed. This data along with detection of CD63+ particles in long-term release studies (fig. 6b) is promising evidence that EV integrity is maintained following processing and release. Notably, it will be important that future studies confirm efficacy of the released biomolecules. In relation to this, it is notable that the entire encapsulation process can be completed in less than 10 min under sterile conditions. This short encapsulation process as well as relatively mild processing conditions, are beneficial for encapsulation of bioactives such as EVs, which are sensitive to both temperature and pH changes. Cytotoxic effects of the microgels were studied using pre-osteoblasts (MC3T3s), cultured in the presence of the systems for 48hrs. Data showed no effect of the microgels on cell survival (fig. 5). Retention of EV structure and lack of toxicity demonstrated the alginate systems to be potential candidates for real clinical applications. However, understanding the kinetics behind release is required for a sustained application.

A comparison in release profiles between the two distinctly structured forms of alginate revealed a notable difference in kinetics. For both systems, no initial burst was observed post *in vitro* immersion. Such observations arise through the uniform distribution of EVs through the matrices (fig 2); as burst release from hydrogels is mainly associated with molecules being embedded in the outer surfaces and payloads escaping during manufacture.[41, 42] Interestingly NTA analysis of elution media (fig. 6c-g) demonstrated that the particles detected were slightly larger, with a longer tail in the distribution on the higher diameter end, than the average initial EV size that was incorporated into both systems. Since no release was detected from control samples of void spheroid microparticles and microgel suspensions, it is hypothesised that the

released particles detected by NTA may be a mixture of single or aggregated EVs that may exit with a small amount of the alginate or that charge groups within the alginate affect the microparticle sizes. Notably, the particles released and the size of encapsulated EVs are larger than the pore-size threshold for alginate gels.[43] As such, ready or rapid release was not expected and this was confirmed in the short-term release study (fig 6a). Since both the EV membrane and alginate molecules are negatively charged, it is unlikely that any electrostatic interactions between the two species has occurred. It is therefore suggested that small pockets of EVs become trapped by the polymer not used during the gelation process. However, it is important to note that future work should look to assess any interaction between the hydrogel structure and vesicle membrane to confirm if any polymer residue is present. Notably, based on NTA results the encapsulation efficiency of the EVs was 95% in the sheared microgel suspension and 99% within the spheroidal microparticles.

To confirm if any of the particles detected by NTA were in fact EVs, an EXO-ELISA was used for the longer-term release study to assay for a vesicle specific protein marker. This analysis demonstrated that there was a cumulative increase in CD63 present in the elution media of both the sheared and spheroidal systems, confirming EVs were being released from both hydrogel structures. Interestingly, kinetics for the sheared systems were almost twice as fast as the spheroids. This likely arises from the physical structuring because, on quantitative evaluation of confocal micrographs, similar numbers of EVs were initially present. For the spheroids, EVs are fully encapsulated in the cross-linked alginate and need to diffuse through the pores of the network; whereas in comparison, since the vesicles are incorporated into both the particles and surrounding aqueous phase, migration through the weakly interacting sheared microgel is more easily achieved. This provides an additional method to control release in conjunction to the previously reported methods for hydrogels: swelling/pore size of the network, any affinity interactions between the bioactive agent and the carrier, and any degradation of the gel.[44, 45] Therefore, such behaviours clearly indicate the potential of the

unique microstructure, to balance effective release of nano-sized therapies whilst engineering in desired rheological characteristics.

This study demonstrates that the existence of these two levels of structuring, 1) the formation of particles via crosslinking of polymers and 2) weak interactions between particles, within the sheared microgel suspensions enhances the release of EVs. Extending this application further, it is presumed that other anionic nano-sized molecules, such as anticancer drugs could take advantage of the sustained release it provides.[46] Furthermore, the nature of these systems also presents the opportunity to increase the degree of control over release, tailoring the proportion of particles incorporated either in or between gelled entities. It is worth mentioning that vesicles are nanoparticles with a negative surface charge, which is due to the structure of their lipid membrane. Therefore, the release profile achieved here might not be applicable for positively charged moieties.

5 Conclusions

Two injectable polymeric systems with different physical structures were systemically investigated for local release of cell-derived extracellular vesicles; with particular emphasis on clinically relevant parameters such as application (injectability), bio-stability/toxicity and release. The integrity of vesicles incorporated into the manufacture of systems via sheared and vibrating nozzle technologies were confirmed using a co-localisation study. Promisingly, even and stable distributions of EVs within both alginate suspensions eliminated burst release, over the initial short-term *in vitro* assays (up to 5h). More specifically, the multi-level structuring achieved by shearing the hydrogel during gelation resulted in interactions between anisotropic particles that exhibited desirable rheological properties (shear thinning and solid-like structures at rest) whilst also enabling sustained release over 12 days. Notably, the technique used to form the microgel particles ultimately dictated the microstructure and resultant release kinetics, with the spheroidal systems releasing a significantly lower concentration of EVs.

While osteoblast-derived vesicles were used as a model in this study, the various properties achievable by applying shear during gelation could also be exploited to deliver other biomolecules with similar size/chemical profiles. In summary, this work highlights the vast potential of physically manipulating biomaterials to enable controlled release of extracellular vesicles, which presents a new approach in regenerative medicine. Future *in vivo* studies will be needed to confirm the bioactivity of released vesicles, as well as evaluating appropriate dosages.

Acknowledgements:

For funding, SC/OD/NN recognise the University of Birmingham's MRC Confidence in Concept scheme and OD the EPSRC E-TERM Landscape Fellowship. IA acknowledges the School of Chemical Engineering, University of Birmingham for doctoral funding. CJK thanks the EU for funding under ERC Starting Grant (Proj. ref: 758064) and Science Foundation Ireland (SFI) under Grant no. SFI/12/RC/2278 (the AMBER Centre). LM acknowledges funding from the EPSRC-NIHR HTC Partnership Award: UNIFY Plus. MT is supported by the NIHR Leicester Biomedical Research Centre. The views expressed are those of the authors and not necessarily those of the NHS, the NIHR or the Department of Health and Social Care.

References

1. Qin, Y., et al., *Bone marrow stromal/stem cell-derived extracellular vesicles regulate osteoblast activity and differentiation in vitro and promote bone regeneration in vivo.* Scientific reports, 2016. **6**.
2. Lee, Y., S. El Andaloussi, and M.J. Wood, *Exosomes and microvesicles: extracellular vesicles for genetic information transfer and gene therapy.* Human molecular genetics, 2012. **21**(R1): p. R125-R134.
3. Franquesa, M., et al., *Update on controls for isolation and quantification methodology of extracellular vesicles derived from adipose tissue mesenchymal stem cells.* Frontiers in immunology, 2014. **5**: p. 525.
4. Zaborowski, M.P., et al., *Extracellular vesicles: Composition, biological relevance, and methods of study.* Bioscience, 2015. **65**(8): p. 783-797.
5. Perez, R., et al., *Therapeutic bioactive microcarriers: co-delivery of growth factors and stem cells for bone tissue engineering.* Acta biomaterialia, 2014. **10**(1): p. 520-530.
6. Yuana, Y., A. Sturk, and R. Nieuwland, *Extracellular vesicles in physiological and pathological conditions.* Blood reviews, 2013. **27**(1): p. 31-39.
7. Davies, O., et al., *Annexin-enriched osteoblast-derived vesicles act as an extracellular site of mineral nucleation within developing stem cell cultures.* Scientific reports, 2017. **7**(1): p. 12639.
8. Xie, H., et al., *Extracellular Vesicle-functionalized Decalcified Bone Matrix Scaffolds with Enhanced Pro-angiogenic and Pro-bone Regeneration Activities.* Scientific Reports, 2017. **7**.
9. Qin, Y., et al., *Exosome: a novel approach to stimulate bone regeneration through regulation of osteogenesis and angiogenesis.* International journal of molecular sciences, 2016. **17**(5): p. 712.
10. Baldari, S., et al., *Challenges and Strategies for Improving the Regenerative Effects of Mesenchymal Stromal Cell-Based Therapies.* International journal of molecular sciences, 2017. **18**(10): p. 2087.

11. Doeppner, T.R., et al., *Concise Review: Extracellular Vesicles Overcoming Limitations of Cell Therapies in Ischemic Stroke.* Stem cells translational medicine, 2017. **6**(11): p. 2044-2052.
12. Vader, P., et al., *Extracellular vesicles for drug delivery.* Advanced drug delivery reviews, 2016. **106**: p. 148-156.
13. Choi, H. and D.S. Lee, *Illuminating the physiology of extracellular vesicles.* Stem cell research & therapy, 2016. **7**(1): p. 55.
14. Li, S.-D. and L. Huang, *Nanoparticles evading the reticuloendothelial system: role of the supported bilayer.* Biochimica et Biophysica Acta (BBA)-Biomembranes, 2009. **1788**(10): p. 2259-2266.
15. Wiklander, O.P., et al., *Extracellular vesicle in vivo biodistribution is determined by cell source, route of administration and targeting.* Journal of extracellular vesicles, 2015. **4**(1): p. 26316.
16. Raghavendra, R., et al., *Diagnostics and therapeutic application of gold nanoparticles.* medicine (bio diagnostics, drug delivery and cancer therapy), 2014. **2**: p. 4.
17. Kearney, C.J. and D.J. Mooney, *Macroscale delivery systems for molecular and cellular payloads.* Nature materials, 2013. **12**(11): p. 1004.
18. Radhakrishnan, J., et al., *Injectable and 3D Bioprinted Polysaccharide Hydrogels: From Cartilage to Osteochondral Tissue Engineering.* Biomacromolecules, 2016. **18**(1): p. 1-26.
19. Khan, F., M. Tanaka, and S.R. Ahmad, *Fabrication of polymeric biomaterials: a strategy for tissue engineering and medical devices.* Journal of Materials Chemistry B, 2015. **3**(42): p. 8224-8249.
20. Szekalska, M., et al., *Alginate: Current use and future perspectives in pharmaceutical and biomedical applications.* International Journal of Polymer Science, 2016. **2016**.
21. Lee, K.Y. and D.J. Mooney, *Alginate: properties and biomedical applications.* Progress in polymer science, 2012. **37**(1): p. 106-126.

22. Farrés, I.F., M. Douaire, and I. Norton, *Rheology and tribological properties of Ca-alginate fluid gels produced by diffusion-controlled method.* Food Hydrocolloids, 2013. **32**(1): p. 115-122.

23. Cooke, M.E., et al., *Structuring of Hydrogels across Multiple Length Scales for Biomedical Applications.* Advanced Materials, 2018. **30**(14): p. 1705013.

24. Farrés, I.F., R. Moakes, and I. Norton, *Designing biopolymer fluid gels: A microstructural approach.* Food Hydrocolloids, 2014. **42**: p. 362-372.

25. Nikravesh, N., et al., *Encapsulation and Fluidization Maintains the Viability and Glucose Sensitivity of Beta-Cells.* ACS Biomaterials Science & Engineering, 2017.

26. Webber, J. and A. Clayton, *How pure are your vesicles?* Journal of extracellular vesicles, 2013. **2**(1): p. 19861.

27. Lötvall, J., et al., *Minimal experimental requirements for definition of extracellular vesicles and their functions: a position statement from the International Society for Extracellular Vesicles*. 2014, Taylor & Francis.

28. Nikravesh, N., et al., *Calcium pre-conditioning substitution enhances viability and glucose sensitivity of pancreatic beta-cells encapsulated using polyelectrolyte multilayer coating method.* Scientific Reports, 2017. **7**.

29. Moulder, K.L., et al., *Vesicle pool heterogeneity at hippocampal glutamate and GABA synapses.* Journal of Neuroscience, 2007. **27**(37): p. 9846-9854.

30. Desrochers, L.M., et al., *Microvesicles provide a mechanism for intercellular communication by embryonic stem cells during embryo implantation.* Nature communications, 2016. **7**: p. 11958.

31. Costes, S.V., et al., *Automatic and quantitative measurement of protein-protein colocalization in live cells.* Biophysical journal, 2004. **86**(6): p. 3993-4003.

32. Dunn, K.W., M.M. Kamocka, and J.H. McDonald, *A practical guide to evaluating colocalization in biological microscopy.* American Journal of Physiology-Cell Physiology, 2011. **300**(4): p. C723-C742.

33. Anitha, A., et al., *Preparation, characterization, in vitro drug release and biological studies of curcumin loaded dextran sulphate–chitosan nanoparticles.* Carbohydrate Polymers, 2011. **84**(3): p. 1158-1164.

34. Matricardi, P., et al., *Preparation and characterization of novel gellan gum hydrogels suitable for modified drug release.* Molecules, 2009. **14**(9): p. 3376-3391.

35. Huang, K.-S., et al., *Electrostatic droplets assisted synthesis of alginate microcapsules.* Drug delivery and translational research, 2011. **1**(4): p. 289-298.

36. Garrec, D.A. and I.T. Norton, *Understanding fluid gel formation and properties.* Journal of Food Engineering, 2012. **112**(3): p. 175-182.

37. Osteikoetxea, X., et al., *Improved characterization of EV preparations based on protein to lipid ratio and lipid properties.* PLoS One, 2015. **10**(3): p. e0121184.

38. Di Rocco, G., S. Baldari, and G. Toietta, *Towards therapeutic delivery of extracellular vesicles: Strategies for in vivo tracking and biodistribution analysis.* Stem cells international, 2016. **2016**.

39. György, B., et al., *Therapeutic applications of extracellular vesicles: clinical promise and open questions.* Annual review of pharmacology and toxicology, 2015. **55**: p. 439-464.

40. Lira, R.B., et al., *Posing for a picture: vesicle immobilization in agarose gel.* Scientific reports, 2016. **6**: p. 25254.

41. Yeo, Y. and K. Park, *Control of encapsulation efficiency and initial burst in polymeric microparticle systems.* Archives of pharmacal research, 2004. **27**(1): p. 1.

42. Allison, S.D., *Analysis of initial burst in PLGA microparticles.* Expert opinion on drug delivery, 2008. **5**(6): p. 615-628.

43. Kearney, C.J., et al., *Switchable release of entrapped nanoparticles from alginate hydrogels.* Advanced healthcare materials, 2015. **4**(11): p. 1634-1639.

44. Orive, G., et al., *Biocompatibility of alginate–poly-l-lysine microcapsules for cell therapy.* Biomaterials, 2006. **27**(20): p. 3691-3700.

45. Lee, S.C., I.K. Kwon, and K. Park, *Hydrogels for delivery of bioactive agents: a historical perspective.* Advanced drug delivery reviews, 2013. **65**(1): p. 17-20.

46. Her, S., D.A. Jaffray, and C. Allen, *Gold nanoparticles for applications in cancer radiotherapy: Mechanisms and recent advancements.* Advanced drug delivery reviews, 2017. **109**: p. 84-101.